Construction and Building Materials 254 (2020) 119323

Contents lists available at ScienceDirect

Construction and Building Materials

journal homepage: www.elsevier.com/locate/conbuildmat

Combined use of recycled powder and recycled coarse aggregate derived from construction and demolition waste in self-compacting concrete

Zhenhua Duan [a,b], Amardeep Singh [a], Jianzhuang Xiao [a,b,*], Shaodan Hou [a]

[a] Department of Structural Engineering, Tongji University, Shanghai, PR China
[b] Key Laboratory of Performance Evolution and Control for Engineering Structures (Tongji University) Ministry of Education, PR China

HIGHLIGHTS

- Hardened properties of self-compacting recycled concrete (SCRC) were analyzed.
- Self-compacting characteristics were maintained when RCA and RP were used.
- The use of FA, SF and RP in SCC mixtures can improve the durability properties.
- Increasing RP content leads to a significant increase in the total porosity.
- RCA and RP have potential to be used as raw material in developing Eco-friendly SCC.

ARTICLE INFO

Article history:
Received 25 January 2020
Received in revised form 16 April 2020
Accepted 22 April 2020
Available online 30 April 2020

Keywords:
Self-compacting concrete
Recycled coarse aggregate (RCA)
Recycled powder (RP)
Fresh properties
Mechanical properties
Durability
Microstructure

ABSTRACT

This study aims to investigate the properties of self-compacting concrete (SCC) with a combined use of recycled coarse aggregate (RCA-0, 25%, 50% and 100% replacement by mass) and recycled powder (RP-10% and 20%), which were both derived from construction and demolition (C&D) waste. Fresh properties were conducted as per EFNARC and porosity was evaluated by using a non-destructive test technique micro X-ray Computer Tomography (X-ray CT). The results showed that SCC mixtures examined in this study all owed excellent flow-ability even when FA was fully replaced with RP. The compressive strength, splitting tensile strength and the resistance to chloride penetration of SCC generally weakened with an increase in the RCA replacement, and the rate of reduction was generally lower when RCA was used no more than 50%. X-ray CT results showed that a higher amount of RP can lead to agglomeration of particles that lead to higher porosity in concrete, which may attribute to the poor durability of SCC with RCA and RP.

1. Introduction

Self-compacting concrete (SCC) has been a research focus for many years because of its ability to remain homogenous during transportation, placing, and after placing and also meet the requirements for strength, volume stability, and durability [1]. The development of SCC is considered as a significant achievement because of its improved properties over normal vibrated concrete (NVC). SCC is a two-phase composite material, where the aggregate phase is dispersed into the paste phase [2]. High powder content, superplasticizers (SP), and viscosity modifying agents (VMA) are the keys to achieve self- compacting features like filling ability, passing ability, and segregation resistance [3]. It is necessary to increase the paste volume in SCC to accommodate aggregates for a better flow-ability and also to consolidate under its weight. However, the increased volume of paste will no doubt impact the cost of SCC and the environment. As per literature, to eliminate 1 billion tons of CO_2 per year, 50% of clinker factor of cement needs to be replaced with material produced with low carbon emissions, which require the use of 1.58 billion tons of supplementary cementitious materials (SCMs) such as fly ash whose global availability is just 800 million tons [4].

Concerning the first concept of cement substitutes, various studies have been performed on SCC with the incorporation of different types of inert filler, pozzolanic, or cementitious additions. Additions such as mineral admixtures (fly ash, silica fume or ground granulated blast furnace slag), marble powder [5], ceramic waste powder [6], granite powder [7], dimensional stone powder [8] and glass powder [9] have well-consolidated practice in cement and concrete industry. One of the most significant additions is

* Corresponding author at: Department of Structural Engineering, Tongji University, Shanghai, PR China.
E-mail address: jzx@tongji.edu.cn (J. Xiao).

https://doi.org/10.1016/j.conbuildmat.2020.119323
0950-0618/

sourced from construction and demolitions (C&D) waste. The production of C&D waste in China is 2 billion tons in the year 2017 [10]. Apart from the production of recycled coarse aggregates (RCA) from C&D waste, a large amount of recycled fine aggregates (RFA) and dust powder (<0.16 mm) are also generated, which account for about 20–50% of the total C&D waste [11] by mass and cannot be utilized effectively at present for their high porosity and impurity content. Another reason being a by-product of RCA and RFA, dust powder is not generally used as a filler material because of low added-value [4,12]. Their utilization has currently become a research focus in China to achieve a sustainable construction industry in the future. Therefore, it is necessary to improve the added value of such recycled materials through physical or chemical approaches, and the most common one is to use the physical force, i.e., by further grinding them into recycled powder (RP) with a certain activity. It is proved that by grinding the α-SiO_2 in RFA/dust powder can be firstly transformed into the more stable β-SiO_2 and then transformed into amorphous SiO_2 [13], which is beneficial to improve the activity. Similarly, $Ca(OH)_2$ and C-S-H in waste concrete can be also converted into more amorphous forms by grinding, leading to higher pozzolanic activity [14].

From a life-cycle perspective, the concrete industry has an energy-extensive consumption because of its super-high demand for natural resources. To alleviate hazards to the environment, it is also necessary to replace cement and aggregate with more sustainable materials. It is generally accepted that replacing natural materials partially or fully by waste materials in concrete reduces the discharge of C&D waste and thus negates the problem of landfills. It has proved that the alternative use of high-quality RCA in concrete can be even accepted up to 100% [15]. Besides, the use of RCA in structural elements, even in high-rise buildings that require improved concrete performance, was also documented [16].

As regards RP produced from C&D waste, though performed weaker than that produced directly from pure cement paste, it was believed to help improve the long-term properties and microstructure of hydration products [17–19]. Schoon et al. [20] and Kwon et al. [21] believed that RP possessed specific hydration activity that could be used to replace limestone as a raw material of cement partially. Topič and Prošek [22] ground old concrete into RP with similar fineness to cement and the results showed that the alternative use of such RP to replace 15% cement could produce higher hydration heat and improvement in flexural strength of concrete as compared with the control mixture. Similar studies conducted by Xiao et al. [18] and Lu et al. [14] showed the replacement of cement by suitable contents of RP could result in the improvement of both mechanical and durability properties. Moreover, it should also be noted that replacing cement with RP and SCMs opens a new horizon for the research and addresses the problem of dumping or landfilling of fine fraction produced from C&D waste.

Currently, few studies have been conducted on the effect of RP in SCC, let alone the combined use of RAC and RP. However, there are still few studies focusing on the combined use of RAC and RP in the properties of SCC. RP used in this study was derived by fine grinding the recycled aggregates from C&D waste. Therefore, this study aims to explore the feasibility of maximum utilization of waste recycled materials both as a partial replacement of coarse aggregate and binder in SCC. Fresh properties such as slump flow, T500, V-funnel and L-box along with mechanical properties such as compression and split tensile strength. Chloride ion penetration, micro X-ray Computer Tomography (X-ray CT) and X-ray diffraction (XRD) were used to investigate the influence on the microstructural properties.

2. Materials and experimental methods

2.1. Materials

PO42.5 cement was used confirming to Chinese standard GB175-2007 [23], while fly ash (FA) and silica fume (SF) were commercially purchased from Jiangyou Power Plant and Huiye Silica Fume Material Co., Ltd in China, respectively. All the recycled material used in this study was derived from waste concrete, which was acquired from a local C&D waste recycling plant which is responsible for recycling the concrete from infrastructure components, the physical properties of RCA is presented in Table 2, which represents a quality index of the old concrete. RP used in this study was obtained through further grinding RFA obtained during the crushing of waste infrastructure components to RCA, by using a cone cavity mill and negative pressure sieves. As per the Chinese Standard GB1596 [24], the powder was obtained as per the requirement where the minimum cumulative content of 45 μm in class I fly ash powder material is 88%. The grain size of RP produced and used in this study satisfies the requirement with a minimum cumulative material 90%, as shown in Fig. 1.

The XRD pattern of RP used in this study is shown in Fig. 2, while a comparison of the chemical compositions between cement and several SCMs like RP, SF, and FA is listed in Table 1. It can be noticed that the main oxide components of RP are almost in-between cement and fly ash. RP mainly comprises quartz (SiO_2) and calcite ($CaCO_3$), showing sand and un-hydrated cement particles.

To assess the pozzolanic activity of the RP, the strength activity index of RP was performed as per the Chinese code GB/T1596 [24], as shown in Fig. 3. Control mortars (cement: sand: water = 1:3:0.57) and mortar with 30% RP cement replacement was prepared and tested for 28-day compressive strength. Results showed that the strength activity index of RP was 80% with a replacement ratio of 30%, illustrating the application potential of RP in concrete. The unit cement volume is the content is the strength potential of the cement by enhancing the contribution of a unit cement content to the strength. It can be seen that by replacing 30% RP with cement the strength decreases from 42.53 MPa to 34.02 MPa and the per unit volume of 'cement' increases by 19%. This allows the other materials to play their full role in strength. This is because the fineness of RP has an excellent effect on the development of strength and can be evenly dispersed in the matrix providing a higher contact area of cement particles and water [25]. The lower value of the compressive strength of mortar at 28 days shows that the overall effect of RP is not similar to the cement, leading to the fact that the unit volume of cement in a mortar with RP remains lower than that of control.

Natural coarse aggregate (NCA) with a maximum size of 12 mm and natural fine aggregate (NFA) with the fineness modulus of 2.71 was used to prepare the reference mixture. RCA with a maximum grain size of 12 mm was obtained from the same recycling plant from where the waste concrete for RP were collected. The physical properties of RCA, NCA, and NFA are shown in Table 2. Fig. 4 shows the particle size distribution of all the aggregate used in this study.

A Poly-carboxylic ether (PCE) based admixture named QS-8020 (Shanghai Qinhe Chemical Co., Ltd., China) in powder form was used as the water reducer in this study.

2.2. Mix design

The mix design method proposed by Su et al. [26] was adopted in this study. Nine mixes with two different mix series, including control, were formulated with a constant water/binder (w/b) ratio of 0.4, as shown in Table 3. Two different

Table 1
Chemical compositions of materials used.

Materials	Chemical compositions (%)										
	SiO_2	CaO	Al_2O_3	Na_2O	P_2O_5	SO_3	K_2O	MgO	TiO_2	MnO	Fe_2O_3
PO42.5	19.9	64.9	4.42	0.08	0.1	2.67	0.79	0.66	0.21	0.1	3
FA	51.7	7.65	23.9	0.58	0.4	0.91	1.4	0.9	1.19	0.07	5.22
SF	98.3	0.36	–	–	–	–	–	–	–	0.01	–
RP	47.9	18.7	12	0.86	0.29	1.41	2.33	2.26	0.82	0.1	6.53

Table 2
Properties of NCA, RCA, and NFA used for the SCC mixes.

Characteristics	NCA	RCA	NFA
Bulk density (kg/m^3)	1438	1220	1497
Specific gravity	2.61	2.59	2.60
Clay content (%)	0.21	1.0	2.0
Aggregate Crushing index (%)	5.1	11.35	–
Water absorption (%)	1	6.53	3.6

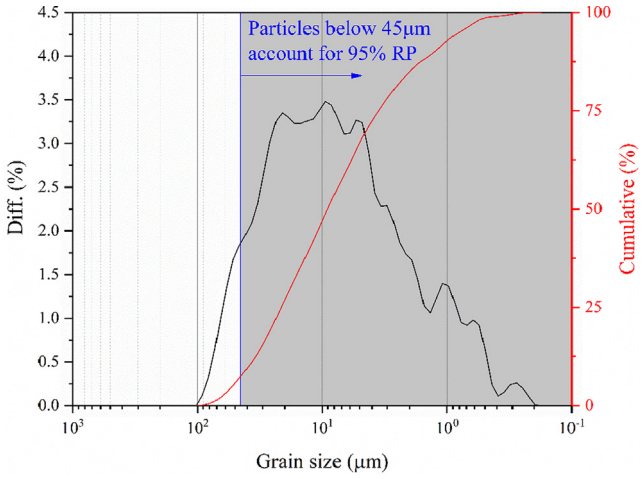

Fig. 1. The particle size distribution of RP.

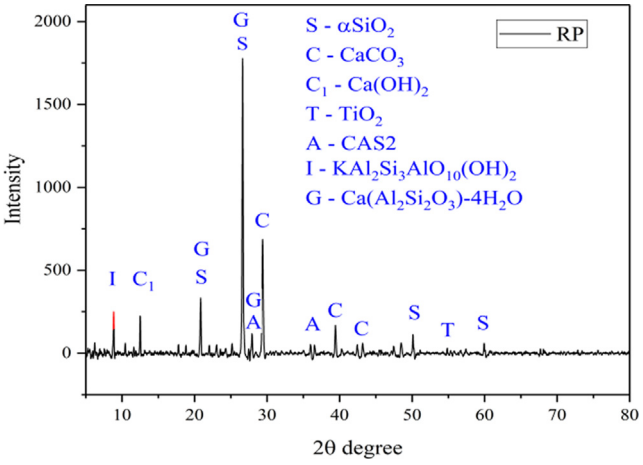

Fig. 2. XRD pattern of RP.

replacement of RP was used to find the optimal combination with RCA. The same amount of SP (0.25% wt. of cementitious materials) was used in all the mixtures to examine the real effect of RCA and powder content on the fresh properties of concrete. A standard tilting drum mixer with dry to wet mixing approach was adopted for mixing concrete. First, coarse and fine aggregates were dry mixed for 30 s, then cementitious materials (cement, SCMs, and RP), and SP were added and further dry mixed for 30 s. Then, 3/4th of the water was added and mixed for another 30 s, and finally, the remaining water was added, and the concrete was mixed thoroughly for the next 1 min for making a homogeneous mix at room temperature of 27 ± 2℃. The RCA were used in saturated surface dry (SSD) condition in order to eliminate the effect of the high-water absorption of RCA. The moisture condition was verified for each batch before mixing the concrete.

2.3. Test methods

2.3.1. Fresh properties

The traditional fresh properties such as slump value, T500 time flow, V-funnel, and L-box were investigated as per the specifications of EFNARC [27] (Table 4) and EN12350-8 [28]. Fig. 5 shows the slump flow and the V-funnel tests in progress. The

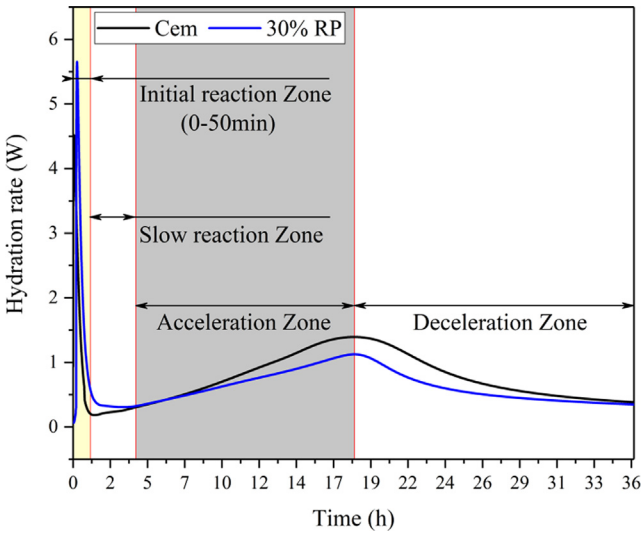

Fig. 3. Hydration rate and heat of hydration for cement paste and paste with 30% RP.

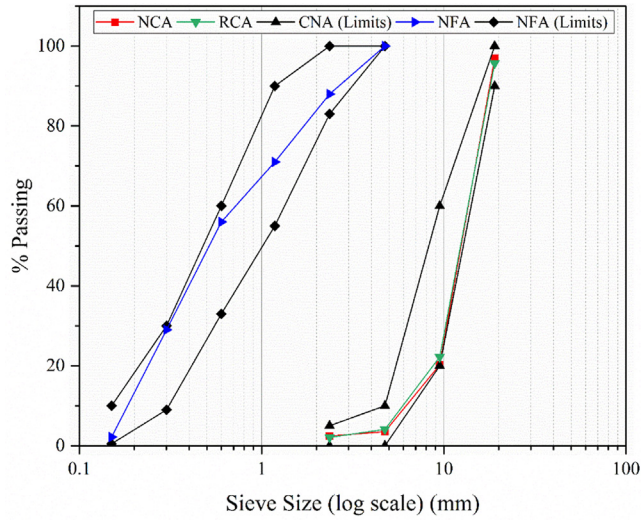

Fig. 4. Particle size distributions of aggregate used in this study.

tests for fresh properties were conducted soon after the mixing protocol and were performed simultaneously to eliminate the effect of time. The repeatability of fresh properties was performed during the mix design trials. After finalizing the mix, the test was done once, in order to see the direct effect of materials on the fresh properties, not the effect of time.

2.3.2. Compressive and splitting tensile test

Compressive test and splitting tensile test were performed as per the Chinese code (GB/T50081-2002) [29] and Indian code (IS:5816–1999) [30], respectively. Test performed in triplets with cubes (100 mm x100mm x100mm) for each of compressive strength and diagonal splitting tensile strength of concrete (Fig. 6) at curing ages of 7, 28, and 56 days.

2.3.3. Chloride ion penetrability

Chloride penetration of SCC was measured following the Chinese code (JTJ270) [31]. Test specimens were exposed to 5% NaCl solution from one exposed face to check the amount of chloride content in concrete. The test was performed using ion-selective AgCl and calomel electrodes on the powder from various depth (0–3 mm, 3–6 mm, 6–9 mm, 9–12 mm, and 12–15 mm) of the sample. A 24-hour wetting and drying cycle was adopted in this test. The relationship was built between the electric potential and the chloride concentration, which follows Fick's second law, as mentioned in Eq. (1).

Table 3
Mix proportions of the experimental program in this study (kg/m^3).

Mix	Notation	Cement	FA	SF	RP	NFA	NCA	RCA	SP
Control	Control	430.5	184.5	0	0	660	780	0	1.53
Series I	C0RP10	430.5	61.5	61.5	61.5	660	780	0	1.53
	C25RP10	430.5	61.5	61.5	61.5	660	585	195	1.53
	C50RP10	430.5	61.5	61.5	61.5	660	390	390	1.53
	C100RP10	430.5	61.5	61.5	61.5	660	0	780	1.53
Series II	C0RP20	430.5	0	61.5	123	660	780	0	1.53
	C25RP20	430.5	0	61.5	123	660	585	195	1.53
	C50RP20	430.5	0	61.5	123	660	390	390	1.53
	C100RP20	430.5	0	61.5	123	660	0	780	1.53

The mix design was taken in mass because the specific gravity of natural coarse aggregate and recycled coarse aggregates are nearly equal.

Table 4
Target limits prescribed by EFNARC.

Property	Notations	Requirements	
		Min.	Max.
Slump flow (mm)	SF1	550	650
	SF2	660	750
	SF3	760	850
T500 (s)	VS1	≤2	
	VS2	>2	
V-funnel (s)	VF1	≤8	
	VF2	9–25	
L-box (ratio)	PA1	≥0.80 with 2 rebars	
	PA2	≥0.80 with 3 rebars	

$$C(x,t) = C_0 + (C_s - C_0)\left[1 - erf\left(\frac{x}{2\sqrt{D_{ap}\cdot t}}\right)\right] \quad (1)$$

where, $C(x,t)$ is the free chloride content at the depth 'x' and time exposure 't(s)'; C_s stands for the surface chloride content (%); C_0 stands for the initial chloride content in concrete (%); $erf(x)$ stands for the error function; D_{ap} stands for the chloride diffusion coefficient having units of 10–12 m^2/s, it can be obtained by fitting the chloride profile with least-square methods.

2.3.4. X-ray diffraction investigation

Microstructural analysis was also performed for a better understanding of the chemical and structural analysis of SCC produced with RCA and RP. Selected mix samples were prepared for each of the testing regimes and the XRD test was conducted on the powder (75 μm) obtained from the broken cubes after testing to analyse the chemical composition. During the test, voltage of 30–60 kV and current of 50–100 mA was employed.

2.3.5. Micro X-ray Computer Tomography

The performance of the composite material directly linked to the constituents materials. A relevant field of research is the establishment of the connection between the characteristic material and the performance parameters, which demands the workflow between these parameters. As it is impossible to differentiate between the changes in the same sample before loading, micro X-ray CT was used for the qualitative and quantitative analysis of the inner structure of SCC with RAC and RP. The test was performed on the samples after 28 days of standard curing. A limited number of samples were investigated for the internal structure. In micro X-ray CT, it was impossible to test the whole cube, so a 50 mm diameter core from an unbroken cube was used to perform the investigation. As shown in Fig. 7 the samples were heated in oven at 102 ± 2℃ for 24 h and then tested.

3. Results and discussion

3.1. Fresh properties

Fig. 8 shows the development trend of fresh properties, including the slump flow, T500, V-funnel and L-box tests, for SCC mixed with different combinations of RCA and RP.

As shown in Fig. 8(a), the variation of SCC in slump flow and T500 when RP maintained at 10%/20% while changing the RCA replacement from 0 to 100% can be observed. With an increase in the replacement ratio of RCA from 0 to 100%, the slump flow - value of SCC with 10% RP decreased by 0.66%, 3.04%, 9% and 14.56%, respectively, whereas the reduction was a bit higher for SCC with 20% RP, about 3.3%, 14.83%, 16.55% and 19.2%, respectively. When RCA was fully used while the alternative use of RP was 10% and 20%, an increase of about 38.89% and 116.67% can be observed in T_{500} value, while the V-funnel result shown in Fig. 8(b) increased by 24.27% and 48.54% accordingly. The adverse effect of RCA content on the fresh properties of SCC can be attributed to its high-water absorption. Firstly, the total amount of attached mortar increased with increased RCA percentage, leading to higher porosity and absorption of water during mixing [32]; Secondly, the increased friction and increased surface area due to increase amount of RCA can influ-

Fig. 5. Slump flow and V-funnel tests of fresh concrete.

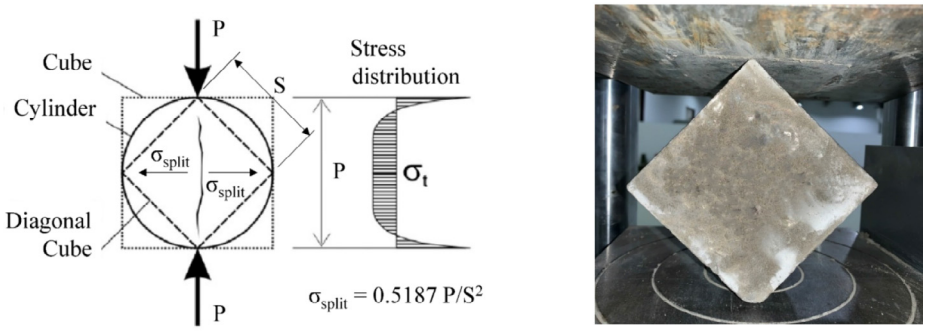

(a) Schematic distribution (b) Specimen under testing

Fig. 6. Test method of splitting tensile strength.

(a) 50mm diameter core (b) X-ray CT machine

Fig. 7. Micro X-ray Computer Tomography test.

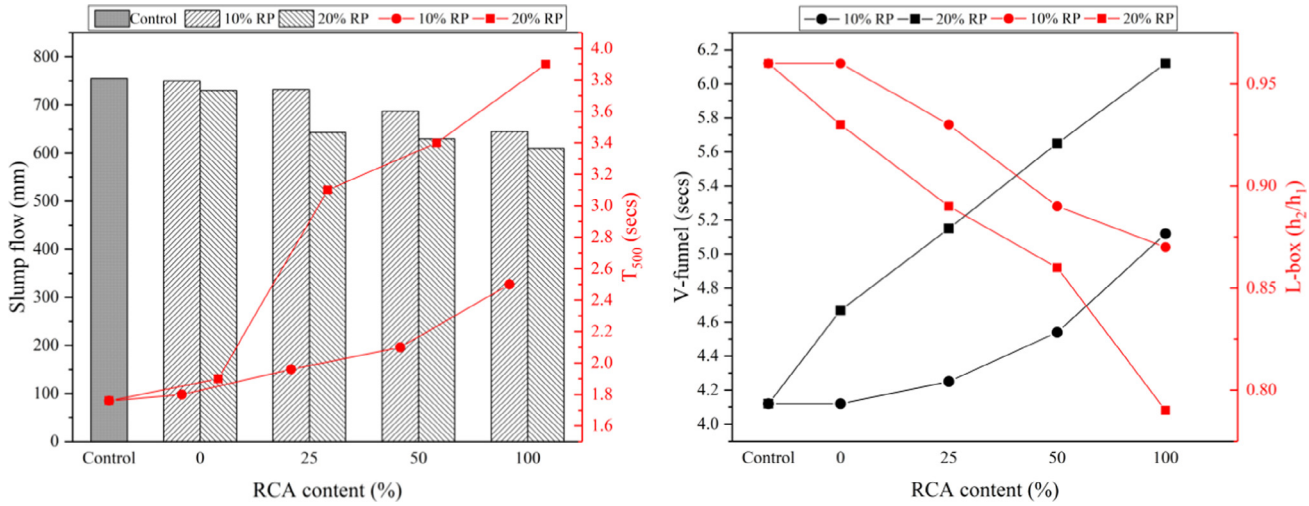

(a) Slump flow and T_{500} tests (b) V funnel and L box tests

Fig. 8. Fresh properties of different SCC mixtures.

ence the interlocking behavior leading to a lower flow-ability [33]. In all the mixes, a Visual Stability Index (VSI) [34] of the fresh concrete was also determined, and all the mixes scored 2, i.e., no perceptible segregation was observed in any mix apart from CON, C0RP10, and C0RP20 which showed the VSI of 1. This showed that the mixes with RCA present a partial tendency of segregation. Whereas, no tendency of segregation is observed with the inclusion of RP.

The results showed that SCC examined in this study show excellent flow-ability even when FA was entirely replaced with RP in all the mixes and fell under the limits prescribed by EFNARC [27]. Similar to T_{500} time, V-funnel and L-box were also used to access the viscosity and passing ability of SCC. These tests typically simulate the placement conditions and time measure value, such as distance, time, and rest time during placement. As per the theory of rheology, the concrete is understood by two parameters, extent of flow and rate of flow. Since the yield stress of conventional SCC and SCC with RCA and RP is a function of replacement percentage and time elapsed after mixing [35]. Based on the empirical fresh properties presented in Fig. 8, no conclusion can be made regarding the effect of RCA on yield stress and plastic viscosity in this study.

As per the grain size distribution of RP, the grain size of RP is lower than that of cement, leading to a higher surface area, which decreases the water film among different particles and increases the interface friction. Besides, the micro-cracks of RP caused by the produce process leads to the higher water absorption than cement. The reduction in the slump value in the concrete mix can be partly attributed to the finer particles and high water absorption of RP, leading to a quicker absorption of the free water required for flow [36]. Even with a controlled amount of powder content, the increase in the surface area can lead to a controllable reduction in the fresh properties of SCC, which is in concordance with the results presented by Wang et al. [37] and Kim et al. [38].

3.2. Mechanical properties

Table 5 shows a comparison of the mechanical properties between the control SCC and SCC prepared with RCA and RP at different curing ages, and a detailed comparison can be noticed in Fig. 9.

As shown in Fig. 9(a), it is as expected that the compressive strength of SCC with and without RCA/RP all increased with curing age. Besides, a gradual reduction can be clearly noticed in the compressive strength of SCC with an increase in the replacement ratio of either RCA or RP, and the reduction is more significant when the replacement ratio of RCA reaches 50%, regardless of the RP dosage; While the reduction in compressive strength is minimal with the replacement of FA alone, about 3.06%, 1.17% and 1.76% for SCC with 10% RP and 5.05%, 3.87% and 10.39% for SCC with 20% RP at 7 days, 28 days and 56 days, respectively. This may be due to the alternative use of RP and SF that can provide enough hydration heat when replacing FA, especially at an early age.

Fig. 9(b) shows the splitting tensile strength of all the SCC mixtures relative to that of the control SCC at 28 days. A reduction in the splitting tensile strength can be observed with the increasing content of RCA/RP. A gradual reduction in the splitting tensile strength was observed at 28 days with the inclusion of RCA, and the reduction were 1%, 18%, 20% and 29% for SCC with 10% RP while 13%, 19%, 25% and 35% for SCC with 20% RP, respectively, at 0, 25%, 50% and 100% RCA replacement. Besides, the rate of reduction was generally lower when RCA was used no more than 50%. The reduction in the splitting tensile strength can be attributed to the different elastic modulus ratio of the new cement mortar, and the old cement mortar can influence the microcrack development around the new interfacial transition zone (ITZ) and old ITZ region of RAC as explained by Xiao et al. [39]. In addition, water of saturated surface dried RCA will bleed, which leads to the higher water to binder ratio around ITZ, resulting in the weaker strength of ITZ. The largest reduction of about 45% was observed in SCC with 100% RCA and 20% RP at 7 days of curing age. After curing for 28 days, the reduction decreased. There is a very small decrease of concrete only with 10% RP after curing for 28 days, showing that concrete with RP has a relative enhancement of strength at later ages, which can be explained by the secondary hydration. The hydration products $Ca(OH)_2$ will react with the reactive element of RP and form $CaCO_3$, leading to the denser microstructure.

3.3. Durability properties

As shown in Fig. 10, the Cl^- permeability of SCC increased with the incorporation of RCA, which is generally accepted due to the presence of residual mortar and defects in RCA. For SCC with alternative use of 10% RP, it can be noticed that the chloride concentration was only a bit higher than that of the control SCC when the incorporation of RCA was no more than 50%. However, for 100% RCA, mix with 20% RP content when compared with mix with 10% RP content, showed an increase in value which is about 2.6, 1.3, 0.8, 0.67 and 0.05 times at 1.5 mm, 4.5 mm, 7.5 mm, 10.5 mm, and 13.5 mm depth respectively. In Series I, the highest chloride concentration was observed in the mix with 100% RCA, whereas the mix with 25% and 50% RCA content showed almost similar results, which can be attributed to the filler effect of RP and the reduction of chloride permeability at convection zone [40]. While for SCC with 20% RP, a gradual increase in chloride content can be observed with an increase in the RCA replacement. Though the high fineness of RP may be helpful to improve the hydration reaction of cement paste and dense the concrete by filling the pores, its overuse may lead to the agglomeration of particles to minimize the interfacial energy between the cementitious particles and the dispersion medium [41]. Such agglomeration effect may hinder the further reaction in SCC, and thus produce unfavourable influence on the chloride ingress behaviour.

3.4. Microstructural analysis

3.4.1. XRD analysis

A comparison of the XRD test results between the control SCC and SCC with a combination use of 100% RCA and 10%/20% RP is shown in Fig. 11, in which αSiO_2 and $CaCO_3$ can be clearly found

Table 5
Mechanical properties of SCC with RCA and RP.

Series No	Mix Notation	Compressive Strength (MPa)			Splitting Tensile Strength (MPa)		
		7d	28d	56d	7d	28d	56d
Control	C0RP0	37.83	42.91	48.41	4.2	4.45	4.88
Series I	C0RP10	36.67	42.41	47.56	3.94	4.44	4.89
	C25RP10	34.61	40.25	45.72	3.57	3.64	4.14
	C50RP10	30.25	36.93	42.52	3.15	3.6	3.81
	C100RP10	29.97	34.85	37.52	2.94	3.2	3.5
Series II	C0RP20	35.92	41.25	43.38	3.82	3.89	4.39
	C25RP20	33.98	40.73	43.77	3.03	3.63	4.16
	C50RP20	28.46	35.97	37.68	2.95	3.34	3.46
	C100RP20	27.89	34.43	36.25	2.43	2.89	3.29

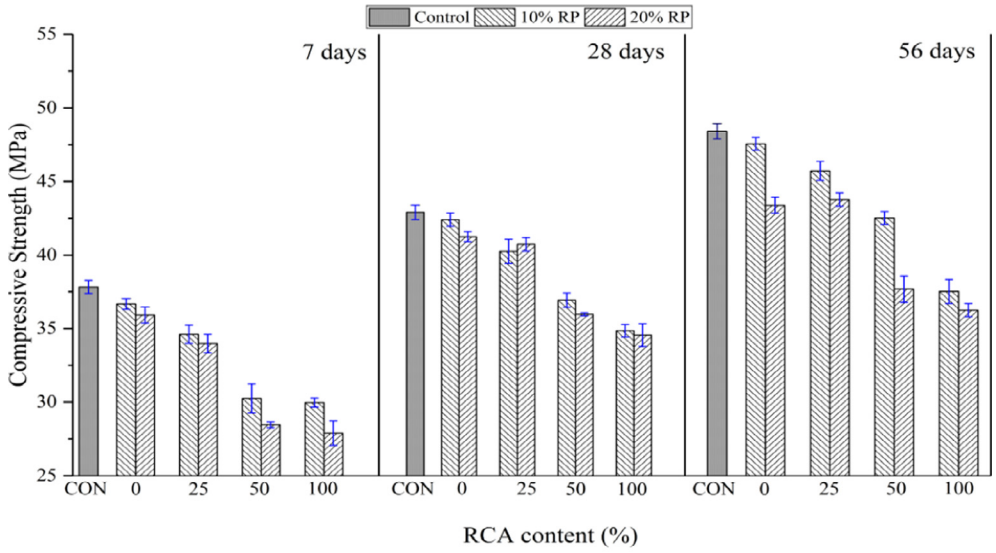

a) Compressive strength

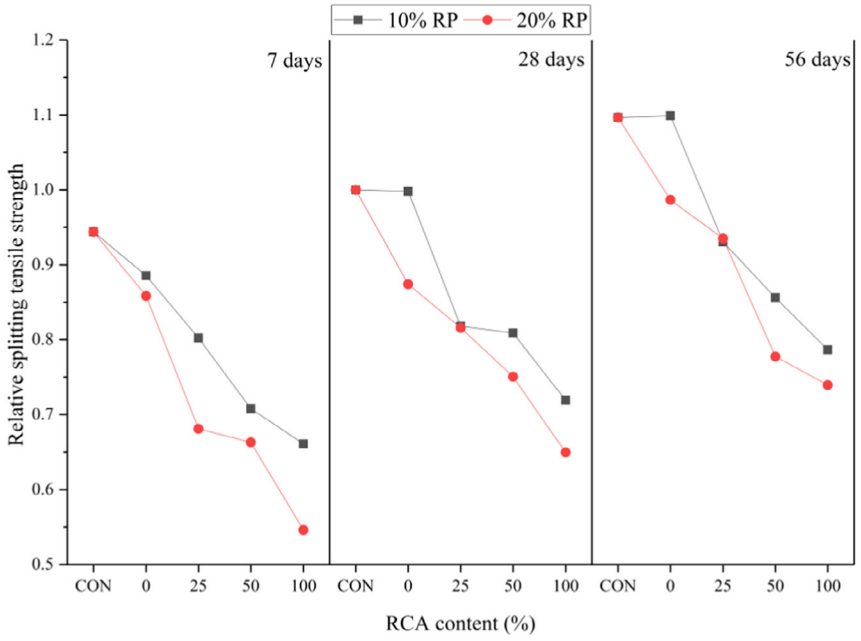

b) Splitting tensile strength of SCC mixtures relative to that of control SCC at 28 days

Fig. 9. Mechanical properties of SCC at 7, 28 and 56 days with different RCA replacement.

in hardened cement paste, and αSiO_2 is found to have relative higher pozzolanic activity while $CaCO_3$ tends to participate during hydration to generate monocarboaluminate ($C_3A{\cdot}CaCO_3{\cdot}11H_2O$). The concentration of SiO_2 and $CaCO_3$ was higher in SCC with 10% RP than that with 20% RP. Besides, small amounts of ettringite were also seen in the XRD pattern of SCC with 10% RP, but not present in that with 20% RP. This can be attributed to the fact that SF and RP were used simultaneously to replace FA in the latter mix as compared with the former one. In the case of the powder produced from the concrete for XRD, the amount of RCA, RP and SF influence the properties of concrete made from these blends. As shown before the oxides of RP are generally between that of cement and FA. As seen from Fig. 11 with the replacement of FA with RP content, there is an increase in the αSiO_2 content in concrete. This increase in αSiO_2 can lead to a higher density of concrete and proves beneficial to the development in the concrete properties. Moreover, the blends of RP, SF and FA, prove that the trade-offs between the positive and negative effect of replacement of RP with SF and FA lead to better effect through optimizing the blends for a mix.

3.4.2. X-ray microtomography

In the case of SCC, the most affected part by using RCA or other recycled materials is durability. Hard synchrotron X-Ray microtomography was used to characterize SCC with the RCA microstructure. Selected mixes with 100% replacement of RCA

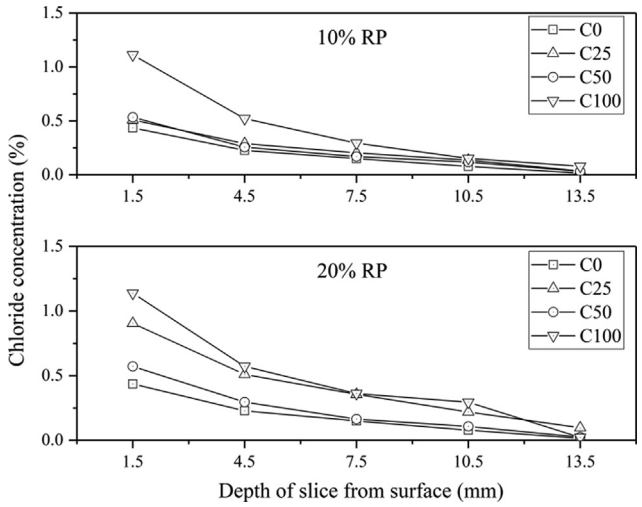

Fig. 10. Chloride concentration at various depths.

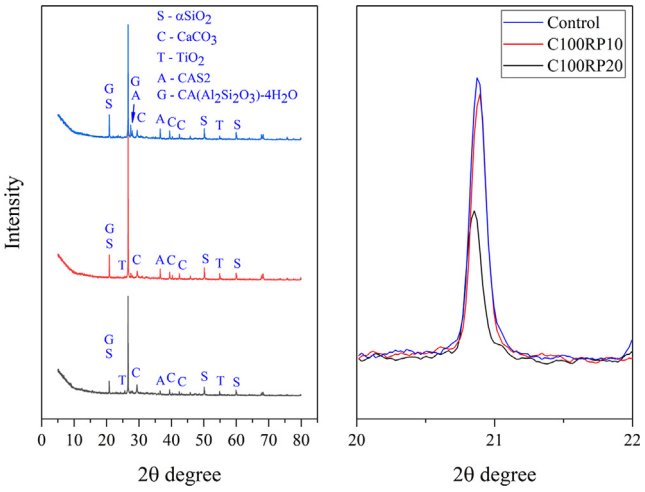

Fig. 11. XRD analysis of concrete.

were tested in X-ray CT to see the effect of RCA along with 10%/20% RP (Control, C100RP10, C100RP20). VGStudio Max was used for analyzing the X-Ray micro-tomography results. Fig. 12(a) shows the tomographic greyscale images with voxel intensity and image after pore segmentation. In Fig. 12(b) the inner circle represents the region of interest (ROI) for calculating the defect (void content).

The defect (void) ratio was calculated by the average defect value of each slice along the axis of the sample. After the processing of X-ray CT slices, the defect volume fraction is presented in Fig. 13(a). Variation of the defect content is mainly attributed to the porosity of concrete, which is affected by the amount of attached mortar and secondary hydration products of RCA and RP. Whereas Fig. 13(b) represents the 3D reconstruction of pores in a sample. It should be noted that the amount of defect also depends on the cutting technique of samples, which can also bring the variation in the analysis of X-ray CT samples [42]. The porosity/inclusion analysis (2.x compatibility) model was used to determine the individual pores, individual pore volume along with sphericity (Sp), compactness (Cc), and surface area (AP) mentioned in Eq. (2) and Eq. (3) [43].

$$S_p = \frac{\pi^{1/3} * (6V)^{2/3}}{A_P} \tag{2}$$

$$C_c = \frac{A_P}{N^2 * T_u} \tag{3}$$

where, V = volume of pores (mm^3), Ap = surface area of pore (mm^2), ϕ = porosity, R = radius of pores (mm), N = number of pores, T_u = Tortuosity

Fig. 14 shows the sphericity and compactness of CON. There is a strong correlation between the sphericity and the compactness of the defect, but no correlation can be seen between the sphericity and the surface area (mm^2). Similar results were obtained in all other mixes. The sphericity increases the compactness of pores but decreases the surface area. The RCA content increases the compactness of the samples except for the sample with 15% RP. This shows that 10% is the optimum dosage of RP for this mix to provide a filler effect, which is due to the secondary hydration reaction [18]. The analysis of the compactness can give us the idea for the volume occupied inside a pore. Whereas, the variation from spherical to conical pores shapes can provide an insight into the additional hydration products formed inside the pores during the hydration stage. Results indicate that the pores in SCC with RCA and RP are neither completely spherical nor cubical. Moreover, with an increase in the surface area, the pore shape tended to deviate from the spherical shape, indicating that pores became non-spherical [43].

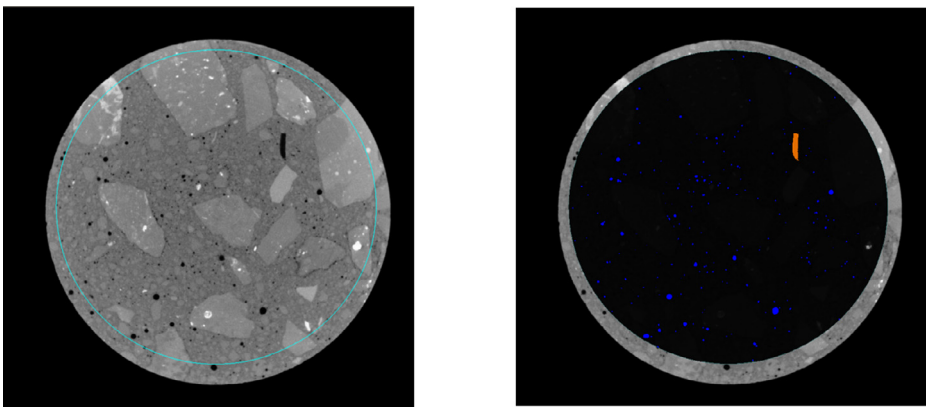

Fig. 12. (a) Grayscale voxelated image (b) Image after pore segmentation.

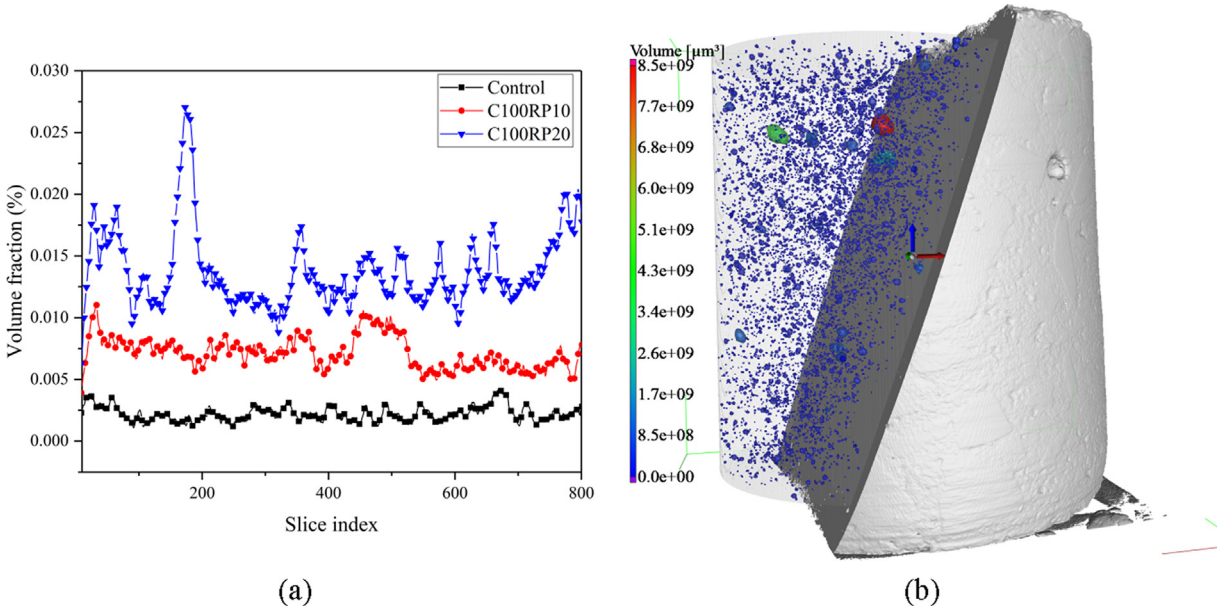

Fig. 13. (a) Variation of the volume fraction of voids slice wise; (b) 3D reconstruction of pores in the control sample.

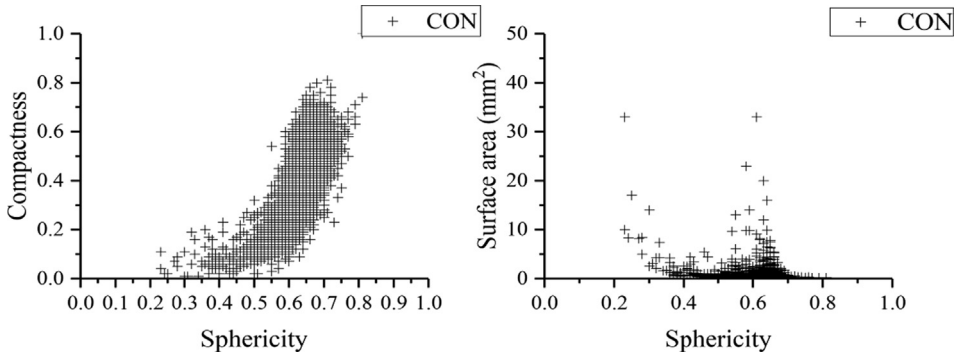

Fig. 14. Relation between Compactness and Surface areas with Sphericity of CON.

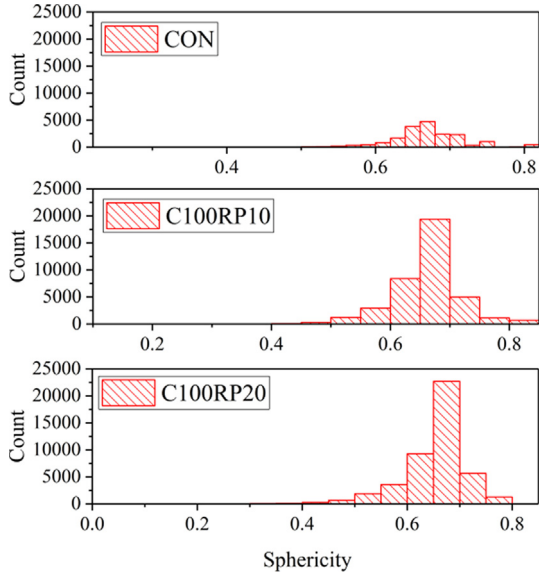

Fig. 15. Sphericity of pores.

Concrete consists of three kinds of pores micropores (1–100 nm), mesopores (100 nm – 0.01 mm), and macro-pores (0.01 mm – 1 cm). Fig. 15 shows the sphericity of pores. The sphericity is plotted in the scale of 0 to 1, where 0 being pores like elongated polygons and 1 represented the perfect circular shape of pores. An exponential behaviour was observed in all samples with a higher number of smaller pores. Although, a higher amount of RP showed higher sphericity, the number of pores per slice in SCC with 20% RP is higher than that of SCC with 10% RP (Fig. 13 (a)). The only reason for the higher porosity can be the agglomeration of finer particles in the cement matrix [41]. Fig. 16 shows the distribution of the micropores in concrete. The amount of micropores in control is less, comparing to concrete with RCA because of the adhered mortar on aggregates. This non-destructive analysis of the calculation of porosity is better than the mercury porosities which is seldom used today because of the environmental issues. The relative total porosity of C100RP10 and C100RP20 is 8.08% and 10.22% of the control mix, respectively. This may be due to the reasons mentioned above, including the filler effect, additional hydration products and the agglomeration of particles due to a higher amount of RP.

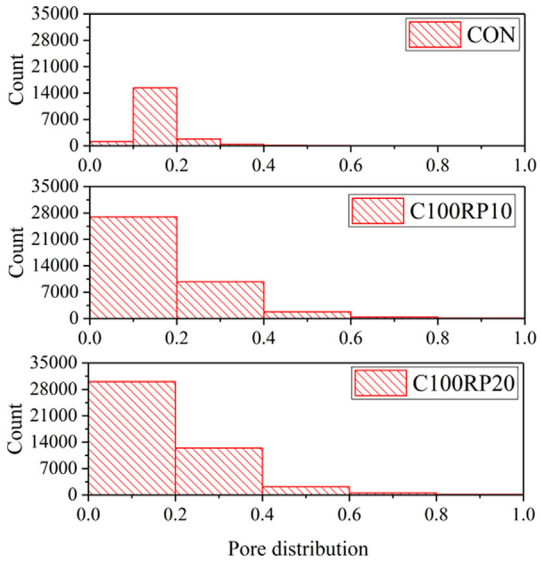

Fig. 16. Micropores distribution in concrete.

4. Conclusions

Based on the various investigations on the fresh and hardened properties of SCC with RP and RCA, the following conclusions can be made:

- Self-compacting concrete (SCC) mixtures examined in this study showed excellent flow-ability even when Fly ash (FA) was fully replaced with recycled powder (RP) in all the mixes. But for SCC with 100% recycled coarse aggregate (RCA), a significant increase in T_{500} time of about 38.89% and 116.67% was observed at 10% and 20% RP respectively. This can be attributed to trade-offs between full replacement of FA by RP, leading to a higher interlocking between the particles in a fresh state and the agglomeration of the particles due to a higher amount of RP. According to the fresh results, increased RP content (agglomeration of the particles) leads to decreased workability.
- The compressive and splitting tensile strength of SCC generally reduced with an increase in the RCA replacement, and the rate of reduction was generally lower when RCA was used no more than 50%. However, at 25% RCA, a minor increase in compressive strength was observed at 28 days when the alternative use of RP was increased from 10% to 20%. Whereas in the case of splitting tensile strength, a higher rate of decrease was observed when 20% RP was used.
- For SCC with an alternative use of 10% RP, though the chloride concentration was much higher than that of the control SCC when RCA was fully used, the concentration value was relatively low when the incorporation of RCA was no more than 50%. While for SCC with 20% RP, a gradual increase in chloride content can be observed with an increase in the RCA replacement. The agglomeration of particles may be a cause for the higher chloride content in the mixes with a higher amount of RP.
- X-ray CT results showed that a higher amount of RP can lead to agglomeration of particles that lead to higher porosity in concrete, which may attribute to the poor durability of SCC with RCA and RP.

It should be emphasized here that the experimental parameters adopted in the study and the relevant conclusions are only valid for the investigated SCC mixes with RCA and RP with the specific material properties and the arrangements for the current experimental study. The effects of the other material properties on the SCC with RCA and RP calls for more efforts. The type and different blends of waste powders from different sources with various particle distributions in SCC with RCA are encouraged in the future. Besides, the effect on the microstructural behavior will be evaluated in-depth.

CRediT authorship contribution statement

Zhenhua Duan: Methodology, Supervision, Writing - review & editing. **Amardeep Singh:** Investigation, Writing - original draft, Writing - review & editing. **Jianzhuang Xiao:** Conceptualization, Methodology, Supervision, Writing - review & editing, Funding acquisition. **Shaodan Hou:** Writing - review & editing.

Declaration of Competing Interest

The authors declare that they have no known competing financial interests or personal relationships that could have appeared to influence the work reported in this paper.

Acknowledgment

This research was funded by the National Natural Science Foundation of China [grant number 51708419]; the joint research project between NSFC and PSF funded by the National Natural Science Foundation of China [grant number 51661145023], and also supported by the Fundamental Research Funds for the Central Universities.

References

[1] L. Wu, C. Shi, Z. Wu, K. Lv, A review on mixture design methods for self-compacting concrete, Constr. Build. Mater. 84 (2015) 387–398, https://doi.org/10.1016/j.conbuildmat.2015.03.079.
[2] I. Topcu, F. Kocataşkin, A two-phase composite materials approach to the workability of concrete, Cem. Concr. Compos. 17 (1995) 319–325, https://doi.org/10.1016/0958-9465(95)00026-9.
[3] R. Gaimster, N. Dixon, Self-compacting concrete, Adv. Concr. Technol. 1 (2003) 1–23, https://doi.org/10.1016/B978-075065686-3/50295-0.
[4] K.L. Lin, B.Y. Chen, C.S. Chiou, A. Cheng, Waste brick's potential for use as a pozzolan in blended Portland cement, Waste Manage. Res. 28 (2010) 647–652, https://doi.org/10.1177/0734242X09355853.
[5] E. Güneyisi, M. Gesoğlu, E. Özbay, Effects of marble powder and slag on the properties of self compacting mortars, Mater. Struct. Constr. 42 (2009) 813–826, https://doi.org/10.1617/s11527-008-9426-2.
[6] L. Ferrara, P. Deegan, A. Pattarini, M. Sonebi, S. Taylor, Recycling ceramic waste powder: effects its grain-size distribution on fresh and hardened properties of cement pastes/mortars formulated from SCC mixes, J. Sustain. Cem. Mater. 8 (2019) 145–160, https://doi.org/10.1080/21650373.2018.1564396.
[7] D.M. Sadek, M.M. El-Attar, H.A. Ali, Reusing of marble and granite powders in self-compacting concrete for sustainable development, J. Clean. Prod. 121 (2016) 19–32, https://doi.org/10.1016/j.jclepro.2016.02.044.
[8] A. Rana, P. Kalla, H.K. Verma, J.K. Mohnot, Recycling of dimensional stone waste in concrete: A review, J. Clean. Prod. 135 (2016) 312–331, https://doi.org/10.1016/j.jclepro.2016.06.126.
[9] M. Liu, Incorporating ground glass in self compacting concrete, Constr. Build. Mater. 25 (2011) 919–925, https://doi.org/10.1016/j.conbuildmat.2010.06.092.
[10] J. Wang, H. Wu, V.W.Y. Tam, J. Zuo, Considering life-cycle environmental impacts and society's willingness for optimizing construction and demolition waste management fee: An empirical study of China, J. Clean. Prod. 206 (2019) 1004–1014, https://doi.org/10.1016/j.jclepro.2018.09.170.
[11] Vázquez, E., Progress of recycling in the built environment: final report of the RILEM Technical Committee 217-PRE, 8 Springer Science & Business Media, 2012.
[12] H. Li, L. Dong, Z. Jiang, X. Yang, Z. Yang, Study on utilization of red brick waste powder in the production of cement-based red decorative plaster for walls, J. Clean. Prod. 133 (2016) 1017–1026, https://doi.org/10.1016/j.jclepro.2016.05.149.
[13] X. Yu, R. Li, X. Dong, G. Li, S. Zhang, Effect of mechanical force grinding on the properties of recycled powder, J. Synth. Cryst. 46 (2017) 688–692.
[14] J. Lu, B. Zhan, Z. Duan, C. Poon, Using glass powder to improve the durability of architectural mortar prepared with glass aggregates, Mater. Des. 135 (2017) 102–111, https://doi.org/10.1016/j.matdes.2017.09.016.

[15] P. Gonçalves, J.D. Brito, Recycled aggregate concrete (RAC) – comparative analysis of existing specifications, Mag. Concr. Res. 62 (2010) 339–346, https://doi.org/10.1680/macr.2008.62.5.339.
[16] J. Xiao, C. Wang, T. Ding, A. Akbarnezhad, A recycled aggregate concrete high-rise building: Structural performance and embodied carbon footprint, J. Clean. Prod. 199 (2018) 868–881, https://doi.org/10.1016/j.jclepro.2018.07.210.
[17] Z. Shui, D. Xuan, H. Wan, B. Cao, Rehydration reactivity of recycled mortar from concrete waste experienced to thermal treatment, Constr. Build. Mater. 22 (2008) 1723–1729, https://doi.org/10.1016/j.conbuildmat.2007.05.012.
[18] J. Xiao, Z. Ma, T. Sui, A. Akbarnezhad, Z. Duan, Mechanical properties of concrete mixed with recycled powder produced from construction and demolition waste, J. Clean. Prod. 188 (2018) 720–731, https://doi.org/10.1016/j.jclepro.2018.03.277.
[19] Z. Duan, S. Hou, J. Xiao, A. Singh, Rheological properties of mortar containing recycled powders from construction and demolition wastes, Constr. Build. Mater 237 (2020) 117622, https://doi.org/10.1016/j.conbuildmat.2019.117622.
[20] J. Schoon, K. De Buysser, I. Van Driessche, N. De Belie, Fines extracted from recycled concrete as alternative raw material for Portland cement clinker production, Cem. Concr. Compos. 58 (2015) 70–80, https://doi.org/10.1016/j.cemconcomp.2015.01.003.
[21] E.H. Kwon, Y.J. Lee, G.H. Cho, C.P. Dong, Analysis on calcination of cementitous powder of waste concrete for raw cement, Adv. Mater. Res., Trans Tech Publ (2014) 267–271.
[22] J. Topič, Z. Prošek, Hydration process and mechanical properties of cement paste with recycled concrete powder and silica sand powder, Acta Polytech. CTU Proc. 13 (2017) 125, https://doi.org/10.14311/APP.2017.13.0125.
[23] GB175-2007, Common Portland cement, Beijing, China, 2007.
[24] GB/T 1596-2017. Fly ash used for cement and concrete, China, China Standard Press, Beijing, China, 2017.
[25] Z. Duan, S. Hou, J. Xiao, B. Li, Study on the essential properties of recycled powders from construction and demolition waste, 253 (2020). doi:10.1016/j.jclepro.2019.119865.
[26] N. Su, K.C. Hsu, H.W. Chai, A simple mix design method for self-compacting concrete, Cem. Concr. Res. 31 (2001) 1799–1807, https://doi.org/10.1016/S0008-8846(01)00566-X.
[27] EFNARC, The European Guidelines for Self-Compacting Concrete: Specification, Production and Use, International Bureau for Precast Concrete (BIBM), 2005.
[28] BS EN 12350-8, Testing fresh concrete. Part 8: Self-compacting concrete - Slump-flow test Br. Stand., 2008.
[29] GB/T50081-2002: Standard for test method of mechanical properties on ordinary concrete. China Architecture & Building Press, 2003, n.d.
[30] BIS IS 5816–1999 (Reaffirmed 2004) Splitting tensile strength of concrete - Method of test, 2004.
[31] JTJ270, Testing code of concrete for port and watering engineering, 2011.
[32] J. Montero, S. Laserna, Influence of effective mixing water in recycled concrete, Constr. Build. Mater. 132 (2017) 343–352, https://doi.org/10.1016/j.conbuildmat.2016.12.006.
[33] M. Behera, A.K. Minocha, S.K. Bhattacharyya, Flow behavior, microstructure, strength and shrinkage properties of self-compacting concrete incorporating recycled fine aggregate, Constr. Build. Mater. 228 (2019) 116819, https://doi.org/10.1016/j.conbuildmat.2019.116819.
[34] E.P. Koehler, D.W. Fowler, Summary of concrete workability test methods, 2003.
[35] I. González-Taboada, B. González-Fonteboa, J. Eiras-López, G. Rojo-López, Tools for the study of self-compacting recycled concrete fresh behaviour: Workability and rheology, J. Clean. Prod. 156 (2017) 1–18, https://doi.org/10.1016/j.jclepro.2017.04.045.
[36] A. Singh, S. Arora, V. Sharma, B. Bhardwaj, Workability retention and strength development of self-compacting recycled aggregate concrete using ultrafine recycled powders and silica fume., J. Hazardous, Toxic, Radioact. Waste. 23 (2019) 4019016, https://doi.org/10.1061/(ASCE)HZ.2153-5515.0000456.
[37] N. Wang, K.F. Zhang, Y. Yao, Q.Y. Cui, P.Z. Huang, T.M. Deng, Performance of recycled pulverized fodder of construction waste with different particle size, Bull. Chinese Ceram. Soc. 34 (2015) 277–279.
[38] Y.J. Kim, Y.W. Choi, J.K. Yong, Y.W. Choi, Utilization of waste concrete powder as a substitution material for cement, Constr. Build. Mater. 30 (2012) 500–504, https://doi.org/10.1016/j.conbuildmat.2011.11.042.
[39] J. Xiao, W. Li, D.J. Corr, S.P. Shah, Simulation study on the stress distribution in modeled recycled aggregate concrete under uniaxial compression, J. Mater. Civ. Eng. 25 (2013) 504–518, https://doi.org/10.1061/(ASCE)MT.1943-5533.0000598.
[40] Z. Ma, W. Li, H. Wu, C. Cao, Chloride permeability of concrete mixed with activity recycled powder obtained from C&D waste, Constr. Build. Mater. 199 (2019) 652–663, https://doi.org/10.1016/j.conbuildmat.2018.12.065.
[41] Y. Zhang, X. Kong, L. Gao, Y. Bai, Characterization of the mesostructural organization of cement particles in fresh cement paste, Constr. Build. Mater. 124 (2016) 1038–1050, https://doi.org/10.1016/j.conbuildmat.2016.08.143.
[42] É. Lublóy, D. Ambrus, K. Kapitány, Á. Barsi, Air Void distribution of asphalts determined by computed tomography, Period. Polytech. Civ. Eng. 59 (2015) 503–510, https://doi.org/10.3311/PPci.7608.
[43] A.K. Chandrappa, K.P. Biligiri, Relationships between structural, functional, and X-Ray microcomputed tomography parameters of pervious concrete for pavement applications, Transp. Res. Rec. 2629 (2017) 51–62, https://doi.org/10.3141/2629-08.